Dinuclear Copper(II) and Mixed-Valence Copper(II)-Copper(I) Complexes of 34-Membered Macrocyclic Ligands (H_2M1, H_2M2) Capable of Forming Endogenous Phenolate and Pyridazino Bridges. X-ray Crystal Structures of the Dinuclear Copper(II) Complexes $[Cu_2M1][BF_4]_2 \cdot H_2O$ and $[Cu_2M2][BF_4]_2 \cdot CH_3OH$, Which Exhibit a Remarkable Ligand Twist

Santokh S. Tandon, Laurence K. Thompson,* and John N. Bridson

Department of Chemistry, Memorial University of Newfoundland, St. John's, Newfoundland, Canada A1B 3X7

Received May 7, 1992

The synthesis, spectroscopic, magnetic, and electrochemical properties of a series of dinuclear copper(II) and mixed-valence copper(II)-copper(I) complexes with the 34-membered macrocyclic ligands H_2M1 and H_2M2 are described. The complexes $[Cu_2(L)]X_2$ (L = M1, X = BF_4 (I), ClO_4 (II); L = M2, X = BF_4 (III), ClO_4 (IV)) are formed by the template condensation of 2,6-diformyl-4-(R)-phenol (2 equiv) (R = CH_3, M1; R = tBu, M2) with 3,6-bis((aminoethyl)thio)pyridazine (2 equiv) in the presence of copper(II) salt. The single crystal X-ray structures of $[Cu_2(M1)](BF_4)_2 \cdot H_2O$ (I) and $[Cu_2(M2)](BF_4)_2 \cdot CH_3OH$ (III) have been determined. I crystallized in the monoclinic system, space group $C2/c$ with a = 38.80 (2) Å, b = 12.618 (6) Å, c = 18.366 (8) Å, β = 112.42 (4)°, and Z = 4. Refinement by full-matrix least-squares techniques gave final residuals R = 0.081 and R_w = 0.058. III recrystallized in the triclinic system, space group $P\bar{1}$ with a = 14.194 (3) Å, b = 15.887 (3) Å, c = 12.240 (3) Å, α = 107.54 (2)°, β = 113.22 (2)°, γ = 82.44 (2)°, and Z = 2. Refinement by full-matrix least-squares techniques gave final residuals R = 0.059 and R_w = 0.050. A macrocyclic ligand twist (~150°) leads to significant distortion at the phenoxide-bridged dicopper centers and brings the pyridazine rings into a position for weak axial contact. Variable-temperature magnetic measurements indicate strong antiferromagnetic coupling ($-2J$ = 560-750 cm^{-1}) for I-IV. Two quasireversible one-electron redox steps are observed (cyclic voltammetry) at -0.08 to -0.1 V and -0.64 to -0.67 V (vs SCE), corresponding to the formation of Cu(II)-Cu(I) and Cu(I)-Cu(I) species, respectively. A series of mixed-valence (Cu(II)-Cu(I)) species has been generated by controlled potential electrolysis of I-IV and characterized by EPR spectroscopy.

Introduction

The 2:2 macrocyclic ligands derived by template condensation of 2,6-diformyl-4-(R)-phenol and 2,6-diacetyl-4-(R)-phenol (R = Me, tBu) with various simple aliphatic and aromatic diamines produces dinuclear macrocyclic complexes in which the chelate ring size created by adjacent imine nitrogen groups falls in the range 5-7.[1-20] The introduction of longer diamines with extra ligand functionality, e.g. with 2-hydroxy-1,3-diaminopropane, 3-hydroxy-1,5-diaminopentane, and 2,6-diaminomethyl-4-methylphenol, has produced related macrocyclic ligands capable of incorporating four and even six metal centers,[21-27] by involving the alkoxo groups as ligands. Our continuing interest in polynucleating open chain and macrocyclic ligands led us to explore the possibility of generating macrocyclic ligands incorporating the familiar 2,6-diiminophenol residues and also heterocyclic diazine fragments, e.g. pyridazines, which have been shown on numerous occasions to generate dinuclear complexes.[28-35]

* Author to whom correspondence should be addressed.

(1) Pilkington, N. H.; Robson, R. *Aust. J. Chem.* **1970**, *23*, 2225.
(2) Okawa, H.; Kida, S. *Bull. Chem. Soc. Jpn.* **1972**, *45*, 1759.
(3) Addison, A. W. *Inorg. Nucl. Chem. Lett.* **1976**, *12*, 899.
(4) Hoskins, B. F.; McLeod, N. J.; Schaap, H. A. *Aust. J. Chem.* **1976**, *29*, 515.
(5) Gagné, R. R.; Koval, C. A.; Smith, T. J. *J. Am. Chem. Soc.* **1977**, *99*, 8367.
(6) Lambert, S. L.; Hendrickson, D. N. *Inorg. Chem.* **1979**, *18*, 2683.
(7) Gagné, R. R.; Koval, C. A.; Smith, T. J.; Cimolino, M. C. *J. Am. Chem. Soc.* **1979**, *101*, 4571.
(8) Gagné, R. R.; Henling, L. M.; Kistenmacher, T. J. *Inorg. Chem.* **1980**, *19*, 1226.
(9) Mandal, S. K.; Nag, K. *J. Chem. Soc., Dalton Trans.* **1983**, *2429*.
(10) Long, R. S.; Hendrickson, D. N. *J. Am. Chem. Soc.* **1983**, *105*, 1513.
(11) Mandal, S. K.; Nag, K. *J. Chem. Soc., Dalton Trans.* **1984**, *2141*.
(12) Carlisle, W. D.; Fenton, D. E.; Roberts, P. B.; Casellato, U.; Vigato, P. A.; Graziani, R. *Transition Met. Chem. (Weinheim, Ger.)* **1986**, *11*, 292.
(13) Mandal, S. K.; Thompson, L. K.; Nag, K.; Charland, J.-P.; Gabe, E. J. *Inorg. Chem.* **1987**, *26*, 1391.
(14) Mandal, S. K.; Thompson, L. K.; Nag, K.; Charland, J.-P.; Gabe, E. J. *Can. J. Chem.* **1987**, *65*, 2815.
(15) Mandal, S. K.; Thompson, L. K.; Nag, K.; *Inorg. Chim. Acta* **1988**, *149*, 247.
(16) Lacroix, P.; Kahn, O.; Gleizes, A.; Valade, L.; Cassoux, P. *Nouv. J. Chim.* **1984**, *8*, 643.
(17) Lacroix, P.; Kahn, O.; Theobald, F.; Leroy, J.; Wakselman, C. *Inorg. Chim. Acta* **1988**, *142*, 129.
(18) Mandal, S. K.; Thompson, L. K.; Newlands, M. J.; Gabe, E. J. *Inorg. Chem.* **1989**, *28*, 3707.
(19) Hendrickson, D. N.; Long, R. C.; Hwang, Y. T.; Chang, H.-R. In *Biological and Inorganic Copper Chemistry*; Karlin, K. D., Zubieta, J., Eds.; Adenine Press: Guilderland, NY, 1985; p 223.
(20) Mandal, S. K.; Thompson, L. K.; Newlands, M. J.; Gabe, E. J. *Inorg. Chem.* **1990**, *29*, 1324.
(21) McKee, V.; Tandon, S. S. *J. Chem. Soc., Chem. Commun.* **1988**, 385.
(22) McKee, V.; Tandon, S. S. *J. Chem. Soc., Chem. Commun.* **1988**, 1334.
(23) McKee, V.; Tandon, S. S. *Inorg. Chem.* **1989**, *28*, 2901.
(24) Tandon, S. S.; Mckee, V. *J. Chem. Soc., Dalton Trans.* **1991**, 221.
(25) Tandon, S. S.; Mckee, V. Unpublished results.
(26) Tandon, S. S.; Thompson, L. K.; Bridson, J. N. *J. Chem. Soc., Chem. Commun.* **1992**, 911.
(27) Hoskins, B. F.; Robson, R.; Smith, P. *J. Chem. Soc., Chem. Commun.* **1990**, 488.
(28) Mandal, S. K.; Thompson, L. K.; Gabe, E. J.; Charland, J.-P.; Lee, F. L. *Inorg. Chem.* **1988**, *27*, 855.
(29) Thompson, L. K.; Mandal, S. K.; Charland, J.-P.; Gabe, E. J. *Can. J. Chem.* **1988**, *66*, 348.
(30) Thompson, L. K.; Mandal, S. K.; Rosenberg, L.; Lee, F. L.; Gabe, E. J. *Inorg. Chim. Acta* **1987**, *133*, 81.
(31) Mandal, S. K.; Thompson, L. K.; Gabe, E. J.; Lee, F. L.; Charland, J.-P.; *Inorg. Chem.* **1987**, *26*, 2384.
(32) Woon, T. C.; McDonald, R.; Mandal, S. K.; Thompson, L. K.; Connors, S. P.; Addison, A. W. *J. Chem. Soc., Dalton Trans.* **1986**, 2381.
(33) Mandal, S. K.; Thompson, L. K.; Newlands, M. J.; Lee, F. L.; LePage, Y.; Charland, J.-P.; Gabe, E. J. *Inorg. Chim. Acta* **1986**, *122*, 199.
(34) Thompson, L. K.; Lee, F. L.; Gabe, E. J. *Inorg. Chem.* **1988**, *27*, 39.
(35) Thompson, L. K.; Mandal, S. K.; Gabe, E. J.; Lee, F. L.; Addison, A. W. *Inorg. Chem.* **1987**, *26*, 657.

0020-1669/93/1332-0032$04.00/0

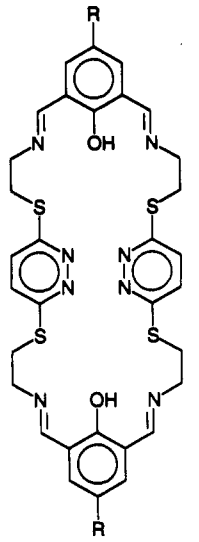

Figure 1. Macrocyclic ligands.

Such a combination could generate a macrocycle with a "high coordination capacity" for metal centers.

In the present study the condensation of 2,6-diformyl-4-(R)-phenol (DFP) (R = Me, tBu) with 3,6-bis(aminoethyl)thio)-pyridazine (PTA) has been carried out in the presence of copper(II) salts involving the weakly coordinating or noncoordinating anions BF_4^- and ClO_4^-, to produce dinuclear copper(II) complexes of the 34-membered macrocyclic ligands H_2M1 and H_2M2 (Figure 1). X-ray structural studies show the familiar, but distorted, equatorial $Cu_2N_4O_2$ dinuclear unit, involving imine nitrogen and phenoxide coordination in the complexes $[Cu_2(M1)](BF_4)_2 \cdot H_2O$ (I) and $[Cu_2(M2)](BF_4)_2 \cdot CH_3OH$ (III). However, unlike normal macrocyclic ligands of this type involving simple diimine linkages between the phenol groups, the ligand adopts an approximately 150° twist, effectively rotating one phenol group relative to the other, leading to a situation where the PTA groups straddle opposite sides of the dinuclear center and generate significant distortion at the copper centers. These complexes exhibit strong antiferromagnetic coupling and redox chemistry involving two one-electron reduction steps at negative potentials (0 to −0.7 V vs SCE). Mixed-valence state (Cu(II)–Cu(I)) species have been generated electrochemically and studied by EPR spectroscopy.

Experimental Section

Safety Note. Perchlorate salts of metal complexes with organic ligands are potentially explosive. Only small amounts of material should be prepared, and these should be handled with caution. The complexes described in this report have, so far, been found to be safe when used in small quantities.

Synthesis of 3,6-Bis((aminoethyl)thio)pyridazine (PTA). Sodium metal (9.5 g, 0.4 mol) was dissolved in degassed absolute ethanol (200 mL) under N_2 and the solution refluxed for 30 min. A solution of 2-aminoethanethiol hydrochloride (22.5 g, 0.2 mol) in warm degassed absolute ethanol (150 mL) was then added, whereupon a white solid (NaCl) separated immediately. The reaction mixture was stirred at 60–70 °C for 30 min and a solution of 3,6-dichloropyridazine (15.0 g, 0.1 mol) in degassed absolute ethanol (100 mL) added dropwise, with stirring, over a period of 1 h. The reaction mixture was then refluxed for 6 h and left at room temperature overnight. The white solid was filtered off, the filtrate concentrated to a volume of about 40 mL, and diethyl ether (50 mL) added. After this was stored in a refrigerator, a pale yellow solid separated, which was filtered, washed with ether, and dried. A second crop of product was obtained from the filtrate by repeating the same procedure. Yield: 87%. Mp: 63–64 °C. Mass spectrum, major mass peaks (m/e (relative intensity)): 231 (1) P, 201 (5), 189 (4), 187 (27) 171 (7), 158 (32), 144 (10), 139 (7), 125 (11), 79 (11). ^{1}H NMR (DMSO-d_6) (δ (relative intensity)): 2.07 (4) (broad singlet, NH_2), 2.82 (4) (triplet, CH_2), 3.24 (4) (triplet, CH_2), 7.44 (2) (singlet, pyridazine CH).

$[Cu_2(M1)](BF_4)_2$ (I). A solution of 2,6-diformyl-4-methylphenol[36] (2 mmol) in hot methanol (50 mL) was added to a solution of $Cu(BF_4)_2$ (4 mmol) in methanol (50 mL) and the mixture refluxed for 15 min. A solution of PTA (2 mmol) in methanol (50 mL) was then added, with continued refluxing, over a period of 10 min. The color of the reaction mixture gradually changed from brown to green. Refluxing was continued for 24 h, the mixture filtered hot, and the green filtrate allowed to stand at room temperature for several days. Olive green needles formed, which were filtered off, washed with methanol and dried under vacuum. Recrystallization by diffusion of ether into a DMF/MeOH solution of the complex produced dark green crystals suitable for X-ray analysis. (Yield: 40%). Anal. Calcd for $[Cu_2(C_{34}H_{34}N_8O_2S_4)](BF_4)_2 \cdot H_2O$: C, 39.51; H, 3.51; N, 10.84; Cu, 12.30. Found: C, 39.81; H, 3.22; N, 10.53; Cu, 12.29.

Complexes II–IV were prepared in a similar manner. Yield of II: 25%. Anal. Calcd for $[Cu_2(C_{34}H_{34}N_8O_2S_4)](ClO_4)_2$: C, 39.23; H, 3.49; N, 10.77; Cu, 12.21. Found: C, 38.82; H, 3.23; N, 10.43; Cu, 12.60. Yield of III: 50%. Anal. Calcd for $[Cu_2(C_{40}H_{46}N_8O_2S_4)](BF_4)_2$: Cu, 11.55. Found: Cu, 11.30. Yield of IV 40%. Anal. Calcd for $[Cu_2(C_{40}H_{46}N_8O_2S_4)](ClO_4)_2 \cdot H_2O$: C, 42.03; H, 4.23; N, 9.80; Cu, 11.12. Found: C, 41.69; H, 3.76; N, 9.50; Cu, 11.16. Crystals of III suitable for X-ray analysis were produced by ether diffusion into a DMF/MeOH solution of the complex.

Preparation of Mixed-Valence (Cu(II)/Cu(I)) Compounds. Mixed valence derivatives of I–IV were prepared in a nitrogen atmosphere by constant-potential electrolysis of the dicopper(II) complexes (0.03–0.04 g in DMF (4mL)) in a three-compartment cell (see physical measurements) at −0.4 V (vs Ag wire). During electrolysis the color of the solution changed from green to dark brown. After completion of the electrolysis (1.5–2.0 h; $n = 1.0 \pm 0.1$), the dark brown solutions were transferred to quartz EPR tubes, under a nitrogen atmosphere.

Physical Measurements. IR and far-IR spectra were recorded with a Mattson Polaris FT infrared spectrometer, and electronic spectra were recorded using a Cary 17 spectrometer. Room-temperature magnetic moments were measured using a Cahn 7600 Faraday magnetic susceptibility system, and variable-temperature magnetic data were obtained in the range 4–300 K using an Oxford Instruments superconducting Faraday susceptometer with a Sartorius 4432 microbalance. A main solenoid field of 1.5 T and a gradient field of 10 T m^{-1} were employed. EPR spectra were recorded with a Bruker ESP 300 X-band spectrometer at 295 and 77 K.

Electrochemical measurements were performed at room temperature in DMF (spectroquality grade dried over molecular sieves) under O_2-free conditions using a BAS CV-27 voltammograph and a Hewlett-Packard 7005B XY recorder. For cyclic voltammetry a three-electrode system was used in which the working electrode was glassy carbon or platinum and the counter electrode was platinum, with a standard calomel (SCE) reference electrode. For constant potential electrolysis, a three-compartment "H" cell was used with a central, 5 mL, working compartment separated from auxiliary and reference compartments by medium-porosity sintered glass frits. The working electrode was a platinum mesh "flag" and the auxiliary electrode was a platinum wire, with a silver wire reference electrode. The supporting electrolyte was either 0.1 M tetraethylammonium perchlorate (TEAP) or tetraethylammonium tetrafluoroborate (TEFB). All potentials are reported vs the standard calomel (SCE) electrode. For cyclic voltammetry all solutions were 10^{-3}–10^{-4} M in complex.

C, H, and N analyses were carried out by Canadian Microanalytical Service, Delta, Canada, and copper was analyzed volumetrically by EDTA titration.

Crystallographic Data Collection and Refinement of the Structures. $[Cu_2(M1)](BF_4)_2 \cdot H_2O$ (I). Crystals of I are deep green. The diffraction intensities of an approximately 0.35 × 0.15 × 0.07 mm crystal were collected with graphite-monochromatized Mo Kα radiation with a Rigaku AFC6S diffractometer using the ω–2θ scan mode to $2\theta_{max} = 45.1°$. A total of 5813 reflections were measured, of which 5702 were unique ($R_{int} = 0.073$) and 1726 were considered significant with $I_{net} > 2.5\sigma(I_{net})$. An empirical absorption correction was applied, using the program DIFABS,[37] which resulted in transmission factors ranging from 0.85 to 1.10. The data were corrected for Lorentz and polarization effects. The cell

(36) Ullman, F.; Brittner, K. *Chem. Ber.* **1909**, *42*, 2539.
(37) Walker, N.; Stuart, D. *Acta Crystallogr.* **1983**, *A39*, 158.

Table I. Summary of Crystallographic Data for $[Cu_2(M1)](BF_4)_2 \cdot H_2O$ (I) and $[Cu_2(M2)](BF_4)_2 \cdot CH_3OH$ (III)

	I	III
empirical formula	$Cu_4C_{68}H_{68}N_{16}O_4B_4F_{16}S_8$	$Cu_2C_{41}H_{49}N_8O_3B_2F_8S_4$
fw	2031.27	1130.83
cryst syst	monoclinic	triclinic
space group	$C2/c$	$P\bar{1}$
a (Å)	38.80 (2)	14.194 (3)
b (Å)	12.618 (6)	15.887 (3)
c (Å)	18.366 (8)	12.240 (3)
α (deg)		107.54 (2)
β (deg)	112.42 (4)	113.22 (2)
γ (deg)		82.44 (2)
volume (Å^3)	8311 (8)	2418.4 (9)
Z	4	2
ρ(calcd) (g cm^{-3})	1.623	1.553
μ (cm^{-1})	12.96	11.23
radiation, λ (Å)	Mo Kα, 0.710 69	Mo Kα, 0.710 69
T (°C)	26	25
$2\theta_{max}$ (deg)	45.1	50.0
no. of obsd reflcns	5813	8610
no. of unique reflcns	1726 ($I > 2.5\sigma(I)$)	3272 ($I > 3.0\sigma(I)$)
GOF	2.03	1.85
R^a	0.081	0.059
$R_w{}^b$	0.058	0.050

^{a} $R = \sum(|F_o| - |F_c|)/\sum(|F_o|)$. ^{b} $R_w = [(\sum w(|F_o| - |F_c|)^2/\sum w(|F_o|)^2]^{1/2}$.

parameters were obtained from a least-squares refinement of the setting angles of nine carefully centered reflections in the range $25.48 < 2\theta < 28.86$.

The structure was solved by direct methods.[38,39] Only the copper, sulfur, phenoxide oxygen, and nitrogen atoms were refined anisotropically. The final cycle of full-matrix least-squares refinement was based on 1726 observed reflections ($I > 2.5\ \sigma(I)$) and 382 variable parameters and converged with $R = 0.081$ and $R_w = 0.058$, with weights based on counting statistics. The maximum and minimum peaks on the final difference Fourier map correspond to +0.52 and −0.48 e/Å^3 respectively. Neutral atom scattering factors[40] and anomalous dispersion terms[41,42] were taken from the usual sources. Both fluoroborates are disordered, one rotationally at a single site and the second rotationally disordered at two sites with 0.5 occupancy. Rigid group modeling gave poor results, and fluorides were therefore located from difference maps and refined positionally. Occupances were adjusted to minimize R values and to maintain reasonable isotropic thermal parameters. All calculations were performed with the TEXSAN[43] crystallographic software package using a VAX 3100 work station. A summary of crystal and other data is given in Table I and atomic coordinates are given in Table II. Hydrogen atom atomic coordinates (Table SI) and thermal parameters (Table SII) are included as supplementary material.

$[Cu_2(M2)](BF_4)_2 \cdot CH_3OH$ (III). Crystals of III are green. The diffraction intensities of an approximately $0.35 \times 0.25 \times 0.15$ mm crystal were collected with graphite-monochromatized Mo Kα radiation with a Rigaku AFC6S diffractometer using the ω–2θ scan mode to $2\theta_{max} = 50.0°$. Data collection and refinement of the structure were carried out as for I. In addition to rotationally disordered fluoroborate ions, the methanol has two principal orientations at the same site. A summary of crystal and other data is given in Table I and atomic coordinates are given in Table III. Hydrogen atom atomic coordinates (Table SIII) and thermal parameters (Table SIV) are included as supplementary material. The copper, sulfur, phenoxide oxygen, nitrogen, and all ligand carbon atoms were refined anisotropically.

Results

The condensation of 2,6-diformyl-4-(R)-phenol (R = Me, tBu) with 3,6-bis((aminoethyl)thio)pyridazine (PTA) in the presence

(38) Gilmore, C. J. *J. Appl. Crystallogr.* **1984**, *17*, 42.
(39) Beurskens, P. T. DIRDIF: Technical Report 1984/1; Crystallography Laboratory: Toernooiveld, 6525 Ed Nijmegen, Netherlands.
(40) Cromer, D. T.; Waber, J. T. *International Tables for X-ray Crystallography*; The Kynoch Press: Birmingham, United Kingdom, 1974; Vol. IV, Table 2.2A.
(41) Ibers, J. A.; Hamilton, W. C. *Acta Crystallogr.* **1974**, *17*, 781.
(42) Cromer, D. T. *International Tables for X-ray Crystallography*; The Kynoch Press: Birmingham, United Kingdom, 1974; Vol. IV, Table 2.3.1.
(43) Texsan-Texray Structure Analysis Package, Molecular Structure Corp., 1985.

Table II. Final Atomic Positional Parameters and B(eq) Values for $[Cu_2(M1)](BF_4)_2 \cdot H_2O$ (I)

atom	x	y	z	B(eq)
Cu(1)	0.87054 (8)	0.0320 (2)	0.0157 (2)	4.2 (1)
Cu(2)	0.88855 (8)	0.2540 (3)	−0.0197 (2)	5.4 (2)
S(1)	0.8740 (2)	−0.0702 (8)	0.1971 (4)	8.4 (5)
S(2)	0.9401 (2)	0.3811 (8)	0.2324 (5)	10.0 (6)
S(3)	0.7863 (2)	−0.0774 (7)	−0.2057 (4)	7.3 (4)
S(4)	0.8397 (3)	0.3707 (7)	−0.2462 (5)	8.7 (5)
F(1)	0.982 (1)	−0.337 (3)	0.044 (3)	6 (1)
F(2)	0.997 (1)	−0.338 (3)	−0.054 (2)	5.2 (9)
F(3)	0.996 (4)	−0.45 (1)	0.034 (7)	7 (2)
F(4)	0.946 (1)	−0.365 (3)	−0.059 (3)	6 (1)
F(5)	1.014 (1)	−0.502 (6)	0.006 (5)	8 (2)
F(6)	0.978 (4)	−0.44 (1)	−0.08 (1)	9 (2)
F(7)	0.990 (4)	−0.30 (1)	−0.00 (1)	6 (2)
F(8)	0.964 (2)	−0.358 (4)	−0.002 (4)	4 (1)
F(9)	1.026 (1)	0.364 (3)	0.738 (2)	9 (1)
F(10)	0.992 (5)	0.37 (1)	0.67 (1)	13 (2)
F(11)	1.018 (2)	0.301 (5)	0.854 (4)	13 (2)
F(12)	0.994 (1)	0.216 (2)	0.726 (2)	10 (1)
F(13)	0.968 (2)	0.351 (7)	0.724 (5)	13 (2)
F(14)	0.293 (1)	0.096 (4)	0.042 (3)	11 (1)
F(15)	0.2976 (7)	−0.013 (2)	−0.064 (1)	8.6 (7)
F(16)	0.282 (1)	0.169 (4)	−0.080 (3)	10 (1)
F(17)	0.304 (1)	0.124 (3)	−0.105 (2)	10 (1)
F(18)	0.271 (1)	0.157 (4)	−0.032 (3)	11 (1)
F(19)	0.328 (1)	0.125 (3)	0.037 (2)	11 (1)
F(20)	0.285 (1)	0.006 (4)	−0.029 (3)	12 (1)
F(21)	0.3367 (7)	0.107 (2)	−0.011 (2)	8.5 (7)
O(1)	0.9068 (3)	0.108 (1)	−0.0155 (7)	3.1 (7)
O(2)	0.8542 (3)	0.179 (1)	0.0122 (7)	3.2 (7)
O(3)	0.889 (1)	−0.327 (3)	−0.075 (2)	9 (1)
N(1)	0.9005 (5)	−0.097 (1)	0.035 (1)	5 (1)
N(2)	0.9076 (5)	0.093 (2)	0.159 (1)	5 (1)
N(3)	0.9232 (5)	0.189 (2)	0.167 (1)	5 (1)
N(4)	0.8869 (5)	0.374 (1)	0.046 (1)	5 (1)
N(5)	0.8191 (5)	−0.017 (2)	−0.003 (1)	4 (1)
N(6)	0.8290 (5)	0.095 (2)	−0.152 (1)	5 (1)
N(7)	0.8388 (5)	0.198 (2)	−0.163 (1)	4 (1)
N(8)	0.9167 (5)	0.300 (2)	−0.087 (1)	5 (1)
C(1)	0.8966 (7)	−0.182 (2)	0.090 (2)	6.7 (7)
C(2)	0.9077 (7)	−0.143 (2)	0.174 (2)	7.3 (8)
C(3)	0.8910 (6)	0.054 (2)	0.205 (1)	4.8 (6)
C(4)	0.8874 (7)	0.129 (2)	0.263 (2)	6.4 (7)
C(5)	0.9022 (7)	0.221 (2)	0.269 (1)	6.6 (7)
C(6)	0.9202 (6)	0.263 (2)	0.224 (1)	4.9 (6)
C(7)	0.9510 (8)	0.397 (2)	0.150 (2)	7.8 (8)
C(8)	0.9219 (8)	0.447 (2)	0.080 (2)	8.3 (8)
C(9)	0.8618 (7)	0.387 (2)	0.078 (1)	4.9 (6)
C(10)	0.8330 (6)	0.312 (2)	0.073 (1)	3.0 (5)
C(11)	0.8300 (6)	0.207 (2)	0.045 (1)	3.4 (5)
C(12)	0.8026 (5)	0.138 (2)	0.050 (1)	2.8 (5)
C(13)	0.7780 (6)	0.179 (2)	0.084 (1)	4.4 (6)
C(14)	0.7835 (5)	0.278 (2)	0.116 (1)	3.0 (5)
C(15)	0.8088 (6)	0.345 (2)	0.110 (1)	4.4 (6)
C(16)	0.7587 (7)	0.319 (2)	0.158 (1)	7.0 (7)
C(17)	0.7965 (6)	0.036 (2)	0.016 (1)	4.4 (6)
C(18)	0.8056 (7)	−0.118 (2)	−0.045 (1)	5.9 (7)
C(19)	0.8163 (7)	−0.132 (2)	−0.117 (2)	6.8 (7)
C(20)	0.8011 (7)	0.046 (2)	−0.216 (2)	5.0 (6)
C(21)	0.7851 (6)	0.103 (2)	−0.286 (1)	5.3 (6)
C(22)	0.7956 (7)	0.200 (2)	−0.298 (2)	6.1 (7)
C(23)	0.8237 (7)	0.244 (2)	−0.231 (2)	5.8 (7)
C(24)	0.8645 (8)	0.431 (2)	−0.154 (2)	9.6 (9)
C(25)	0.9073 (8)	0.411 (2)	−0.117 (2)	8.4 (8)
C(26)	0.9358 (7)	0.228 (2)	−0.108 (1)	5.8 (7)
C(27)	0.9451 (6)	0.127 (2)	−0.090 (1)	3.5 (5)
C(28)	0.9292 (6)	0.063 (2)	−0.048 (1)	3.4 (5)
C(29)	0.9377 (6)	−0.041 (2)	−0.036 (1)	3.7 (5)
C(30)	0.9633 (6)	−0.088 (2)	−0.066 (1)	4.9 (6)
C(31)	0.9761 (6)	−0.026 (2)	−0.109 (1)	5.5 (6)
C(32)	0.9691 (6)	0.079 (2)	−0.122 (1)	4.2 (6)
C(33)	1.0028 (7)	−0.069 (2)	−0.149 (2)	7.9 (8)
C(34)	0.9271 (7)	−0.111 (2)	0.010 (1)	4.9 (6)
B(1)	0.980 (2)	−0.400 (5)	−0.018 (4)	3 (1)
B(2)	1.009 (3)	0.317 (6)	0.784 (4)	6 (2)
B(3)	0.292 (1)	0.098 (5)	−0.032 (3)	10 (1)

^{a} $B_{(eq)} = (8\pi^2/3) \sum_{i=1}^{3} \sum_{j=1}^{3} U_{ij} d_i^* a_j^* \vec{a}_i \cdot \vec{a}_j$.

Table III. Final Atomic Positional Parameters and B(eq) Values for $[Cu_2(M2)](BF_4)_2 \cdot CH_3OH$ (III)

atom	x	y	z	B(eq)
Cu(1)	0.3456 (1)	0.3294 (1)	0.6792 (1)	2.67 (6)
Cu(2)	0.1540 (1)	0.2169 (1)	0.5190 (1)	2.69 (7)
S(1)	0.1039 (3)	-0.0092 (2)	0.4382 (4)	4.8 (2)
S(2)	0.5639 (2)	0.0822 (2)	0.6778 (3)	3.9 (1)
S(3)	-0.0745 (2)	0.4302 (3)	0.5848 (4)	4.7 (2)
S(4)	0.3772 (3)	0.5273 (2)	0.9073 (3)	4.1 (2)
F(1)	0.6267	0.2534	0.3418	20 (2)
F(2)	0.6662	0.2396	0.4430	19 (1)
F(3)	0.532 (1)	0.352 (1)	0.374 (1)	12.4 (4)
F(4)	0.606 (1)	0.3633 (9)	0.554 (1)	10.7 (4)
F(5)	0.585 (2)	0.243 (1)	0.417 (2)	12.8 (6)
F(6)	0.6910 (8)	0.3605 (7)	0.439 (1)	12.3 (4)
F(7)	0.8039	0.1640	0.8117	9.1 (7)
F(8)	0.8738	0.2493	1.0214	7.7 (6)
F(9)	0.9293	0.2105	0.8527	7.1 (7)
F(10)	0.9201	0.1241	0.9806	6.8 (5)
F(11)	0.9710	0.1523	0.9519	5.4 (6)
F(12)	0.7948	0.1567	0.8888	8.8 (9)
F(13)	0.8916	0.2795	0.9897	5.2 (6)
F(14)	0.8551	0.2393	0.8012	8 (1)
F(15)	0.9711	0.1878	0.9129	8.1 (5)
F(16)	0.8545	0.1865	1.0310	8 (1)
F(17)	0.7990	0.1335	0.8304	5.7 (5)
F(18)	0.8314	0.2753	0.9318	6.8 (7)
O(1)	0.2476 (5)	0.2884 (5)	0.5011 (7)	2.5 (3)
O(2)	0.2552 (5)	0.2531 (5)	0.6859 (6)	2.2 (3)
O(3)	0.736 (2)	0.224 (2)	0.144 (3)	15 (1)
O(4)	0.755 (3)	0.180 (2)	0.240 (4)	20 (1)
N(1)	0.0764 (7)	0.1812 (6)	0.3419 (8)	2.6 (4)
N(2)	0.2634 (7)	0.0911 (7)	0.5093 (9)	3.5 (5)
N(3)	0.3639 (8)	0.1117 (6)	0.558 (1)	3.3 (5)
N(4)	0.4641 (6)	0.2719 (6)	0.7831 (8)	2.4 (4)
N(5)	0.0522 (6)	0.2205 (6)	0.5954 (8)	2.4 (4)
N(6)	0.1292 (8)	0.4082 (6)	0.645 (1)	3.2 (5)
N(7)	0.2269 (7)	0.4330 (6)	0.7183 (9)	2.7 (4)
N(8)	0.4063 (6)	0.4162 (6)	0.6433 (8)	2.3 (4)
C(1)	0.2320 (7)	0.3186 (7)	0.408 (1)	1.6 (4)
C(2)	0.2951 (7)	0.3874 (7)	0.422 (1)	1.7 (4)
C(3)	0.2793 (9)	0.4196 (7)	0.323 (1)	2.4 (5)
C(4)	0.1997 (8)	0.3886 (7)	0.206 (1)	2.2 (5)
C(5)	0.1389 (8)	0.3225 (8)	0.194 (1)	2.5 (5)
C(6)	0.1522 (8)	0.2884 (7)	0.293 (1)	2.1 (5)
C(7)	0.1892 (9)	0.4270 (8)	0.103 (1)	2.8 (5)
C(8)	0.090 (1)	0.394 (1)	-0.012 (1)	4.7 (7)
C(9)	0.192 (1)	0.5263 (9)	0.142 (1)	4.7 (7)
C(10)	0.280 (1)	0.3889 (9)	0.060 (1)	4.7 (6)
C(11)	0.0852 (8)	0.2169 (7)	0.267 (1)	2.5 (5)
C(12)	0.0081 (9)	0.1044 (8)	0.285 (1)	3.6 (5)
C(13)	0.065 (1)	0.0163 (9)	0.293 (1)	4.9 (7)
C(14)	0.2344 (9)	0.0136 (9)	0.506 (1)	3.1 (5)
C(15)	0.305 (1)	-0.0459 (8)	0.560 (1)	4.5 (7)
C(16)	0.405 (1)	-0.0253 (8)	0.613 (1)	4.6 (6)
C(17)	0.4320 (9)	0.0567 (8)	0.609 (1)	3.1 (5)
C(18)	0.5673 (8)	0.1911 (8)	0.661 (1)	3.2 (5)
C(19)	0.5666 (8)	0.2659 (8)	0.774 (1)	3.5 (6)
C(20)	0.4575 (8)	0.2287 (7)	0.853 (1)	2.7 (5)
C(21)	0.2683 (8)	0.2156 (7)	0.772 (1)	2.3 (5)
C(22)	0.3646 (8)	0.2052 (7)	0.860 (1)	2.3 (5)
C(23)	0.3751 (8)	0.1635 (8)	0.948 (1)	3.1 (5)
C(24)	0.2905 (9)	0.1331 (8)	0.957 (1)	2.9 (5)
C(25)	0.1966 (9)	0.1471 (8)	0.875 (1)	2.9 (5)
C(26)	0.1821 (8)	0.1865 (7)	0.781 (1)	2.5 (5)
C(27)	0.306 (1)	0.0843 (9)	1.053 (1)	3.6 (6)
C(28)	0.353 (1)	0.149 (1)	1.182 (1)	5.3 (7)
C(29)	0.208 (1)	0.052 (1)	1.044 (1)	7.3 (9)
C(30)	0.383 (1)	0.010 (1)	1.046 (1)	6.2 (8)
C(31)	0.0783 (8)	0.2042 (7)	0.700 (1)	2.7 (5)
C(32)	-0.0562 (8)	0.2442 (8)	0.536 (1)	3.4 (5)
C(33)	-0.0708 (9)	0.3236 (9)	0.483 (1)	4.3 (6)
C(34)	0.0525 (9)	0.4609 (8)	0.666 (1)	3.3 (6)
C(35)	0.071 (1)	0.542 (1)	0.756 (1)	4.4 (7)
C(36)	0.169 (1)	0.5653 (8)	0.828 (1)	4.3 (6)
C(37)	0.248 (1)	0.5080 (9)	0.807 (1)	3.3 (6)
C(38)	0.4322 (9)	0.5562 (8)	0.812 (1)	3.6 (5)
C(39)	0.4810 (8)	0.4784 (7)	0.744 (1)	2.9 (5)
C(40)	0.3761 (8)	0.4295 (7)	0.536 (1)	2.2 (5)
C(41)	0.644 (2)	0.212 (2)	0.151 (3)	23 (1)
B(1)	0.6201	0.3209	0.4504	13 (1)
B(2)	0.8797	0.1920	0.9202	7.0 (5)

[a] $B_{(eq)} = (8\pi^2/3) \sum_{i=1}^{3} \sum_{j=1}^{3} U_{ij} a_i^* a_j^* \vec{a}_i \cdot \vec{a}_j$.

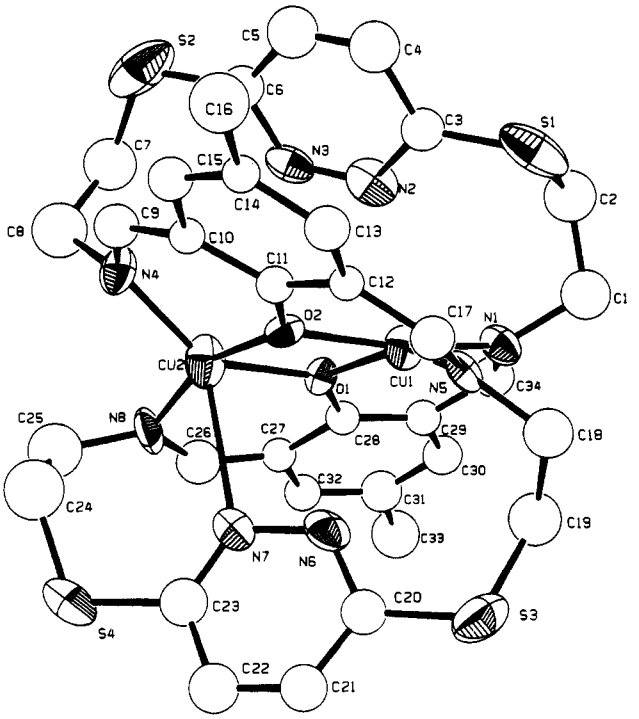

Figure 2. Structural representation of $[Cu_2(M1)]^{2+}$ (cation of I) with hydrogen atoms omitted (40% probability thermal ellipsoids).

of copper(II) salts of weakly coordinating or noncoordinating anions (e.g. ClO_4^-, BF_4^-) results in the formation of 2:2 macrocyclic ligands (M1, M2). These 34-membered macrocycles are potentially decadentate (N_8O_2) ligands, capable of forming endogenous phenolate and pyridazino bridges and possibly binding four metal centers. The involvement of the sulfur atoms as donors could, conceivably, increase the coordination capacity beyond four. However, in the present complexes, the macrocycles coordinate with the familiar N_4O_2, equatorial donor set, to two phenoxide bridged copper(II) centers, but distant axial contacts indicate weak coordination of pyridazine nitrogen atoms as well.

In contrast to this behavior, it the condensation of the 2,6-diformyl-4-(R)-phenols is carried out with PTA in the presence of other copper(II) salts of anions with significant coordinating abilities (e.g. Cl, Br, NO_3, CF_3SO_3), 1:1, 17-membered macrocycles are formed which accommodate two copper centers involving phenoxide and methoxide or anion bridges.[44]

Description of the Structure of $[Cu_2(M1)](BF_4)_2 \cdot H_2O$ (I). The structure of the cation $[Cu_2(M1)]^{2+}$ is shown in Figure 2, and bond lengths and bond angles relevant to the copper coordination spheres are given in Table IV. Each copper atom has four short equatorial contacts to phenoxide oxygen bridging atoms O(1) and O(2) and imine nitrogens N(1), N(5)(Cu(1)), N(4), and N(8)(Cu(2)). These ligand donor atoms form a tetrahedrally distorted N_2O_2 set around each copper center, unlike the situation for the traditional macrocyclic derivatives of this sort, with short (two, three, or four) atom linkages between the imine groups, where the copper centers have close to planar geometries. The dinuclear center itself, (Cu(1), O(1), O(2), Cu(2)) is close to planar (solid angles at O(1) and O(2) of 357.5° and 358.0° respectively) with significant displacements of N(1), N(5), N(4), and N(8) (0.375 (7), -0.855 (7), 1.124 (7), -0.630 (7) Å, respectively) from the Cu(1), Cu(2), O(1), and O(2) plane. One very remarkable feature of the structure, which in no small measure is responsible for the distortion at the copper centers, is the fact that the ligand adopts a 147° twist on coordination. Imine donors N(1) and N(5) lie on one side of the dinuclear center, while N(4) and N(8) lie on the other. The PTA fragments

(44) Tandon, S. S.; Thompson, L. K. Unpublished results.

Table IV. Interatomic Distances (Å) and Angles (deg) Relevant to the Copper Coordination Spheres in $[Cu_2M1][BF]_2 \cdot H_2O$ (I) and $[Cu_2M2][BF]_2 \cdot CH_3OH$ (III).

I		III	
Cu(1)–O(1)	1.96 (1)	Cu(1)–O(1)	2.026 (7)
Cu(1)–O(2)	1.95 (1)	Cu(1)–O(2)	1.917 (7)
Cu(1)–N(1)	1.95 (2)	Cu(1)–N(4)	1.973 (8)
Cu(1)–N(5)	1.99 (2)	Cu(1)–N(8)	1.952 (8)
Cu(1)–N(2)	2.59 (2)	Cu(1)–N(7)	2.281 (9)
Cu(2)–O(1)	1.96 (1)	Cu(2)–O(1)	1.969 (7)
Cu(2)–O(2)	1.90 (1)	Cu(2)–O(2)	1.940 (7)
Cu(2)–N(4)	1.95 (2)	Cu(2)–N(1)	1.943 (9)
Cu(2)–N(8)	2.02 (2)	Cu(2)–N(5)	1.995 (8)
Cu(2)–N(7)	2.69 (2)	Cu(2)–N(2)	2.37 (1)
Cu(1)–Cu(2)	3.017 (5)	Cu(1)–Cu(2)	3.066 (2)
O(1)–Cu(1)–O(2)	77.7 (5)	O(1)–Cu(1)–O(2)	76.7 (3)
O(1)–Cu(1)–N(1)	91.0 (7)	O(1)–Cu(1)–N(7)	89.2 (3)
O(2)–Cu(1)–N(5)	89.9 (7)	O(1)–Cu(1)–N(8)	92.1 (3)
N(1)–Cu(1)–N(5)	105.1 (8)	O(2)–Cu(1)–N(4)	89.8 (3)
O(1)–Cu(1)–N(5)	152.1 (6)	O(2)–Cu(1)–N(7)	81.7 (3)
O(2)–Cu(1)–N(1)	163.9 (7)	N(4)–Cu(1)–N(8)	104.4 (4)
O(1)–Cu(2)–O(2)	78.8 (6)	N(7)–Cu(1)–N(8)	89.4 (3)
O(1)–Cu(2)–N(8)	91.3 (7)	O(1)–Cu(1)–N(4)	132.5 (3)
O(2)–Cu(2)–N(4)	90.2 (7)	O(2)–Cu(1)–N(8)	165.7 (3)
N(4)–Cu(2)–N(8)	107.9 (8)	N(4)–Cu(1)–N(7)	134.2 (3)
O(1)–Cu(2)–N(4)	143.0 (7)	O(1)–Cu(2)–O(2)	77.6 (3)
O(2)–Cu(2)–N(8)	159.7 (7)	O(1)–Cu(2)–N(1)	92.3 (3)
Cu(1)–O(1)–Cu(2)	100.5 (6)	O(2)–Cu(2)–N(5)	86.9 (3)
Cu(1)–O(2)–Cu(2)	103.0 (6)	N(1)–Cu(2)–N(5)	104.9 (4)
		O(2)–Cu(2)–N(2)	81.9 (3)
		N(1)–Cu(2)–N(2)	92.5 (4)
		N(5)–Cu(2)–N(2)	117.1 (3)
		O(1)–Cu(2)–N(2)	92.4 (3)
		O(2)–Cu(2)–N(1)	168.1 (3)
		O(1)–Cu(2)–N(5)	144.5 (3)
		Cu(1)–O(1)–Cu(2)	100.2 (3)
		Cu(1)–O(2)–Cu(2)	105.3 (3)

link N(1) and N(4) and link N(5) and N(8) and so straddle the dinuclear center with the pyridazine nitrogens pointing inward above and below the copper centers. An examination of possible axial contacts reveals two with distances <2.7 Å (Cu(1)–N(2) 2.59 (2) Å, Cu(2)–N(7) 2.69 (2) Å). However the pyridazine ring including N(2) has a dihedral angle of 40.5° with respect to the Cu_2O_2 plane, and so Cu(1)–N(2) is clearly not a significant bonding contact. The geometry at Cu(1) is therefore best described as tetrahedrally distorted square-planar. The dihedral angle of the other pyridazine ring with the Cu_2O_2 plane (96.4°) is closer to 90° and suggests that the Cu(2)–N(7) contact is significant. The Cu(2)–N(7)–C(23) (136 (2)°) and Cu(2)–N(7)–N(6) (104 (1)°) angles, although removed somewhat from the idealized geometry, are also consistent with such a contact. Cu(2), therefore, is considered to have a distorted square-pyramidal geometry, with a weak axial interaction.

A rationalization of the unusual ligand twist can be obtained by considering how the complex might have formed. The reaction involved the initial combination of 2,6-diformyl-4-methylphenol and $Cu(BF_4)_2$ in hot refluxing methanol, which presumably produced a "planar" dinuclear, phenoxide-bridged intermediate (brown) involving terminal aldehyde coordination (Cu_2O_6). The subsequent addition of the diamine (PTA), following the traditional preparation route, clearly does not complete the macrocycle by condensation of its two diamine ends on each side of the dinuclear intermediate. One condensed imine unit is formed, and then, rather than form an unreasonably large and clearly highly strained 13-membered chelate ring around one copper center, the other end of the PTA group spans the dinuclear center and completes its second imine condensation at the other copper atom. This process is repeated on the other side of the dinuclear centers to complete the 34-membered macrocycle and produces an arrangement where the two PTA fragments effectively act as diagonal "straps" between the copper atoms.

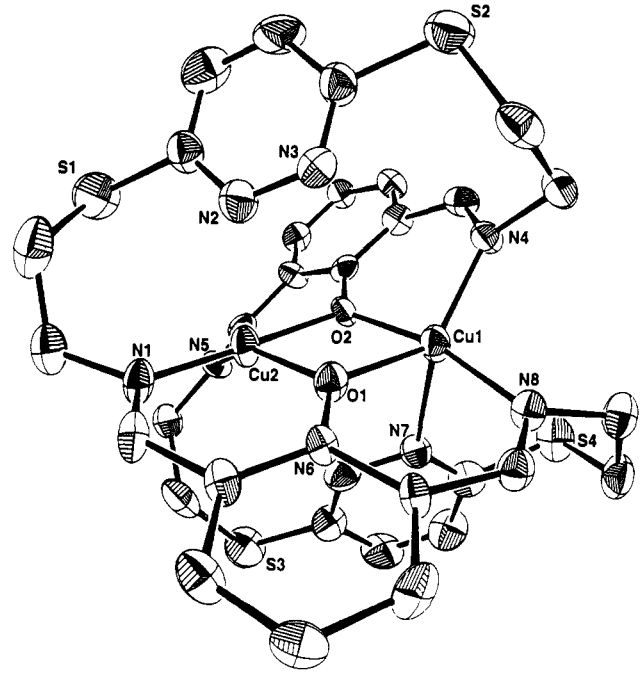

Figure 3. Structural representation of $[Cu_2(M2)]^{2+}$ (cation of III) with hydrogen atoms and *tert*-butyl groups omitted (40% probability thermal ellipsoids).

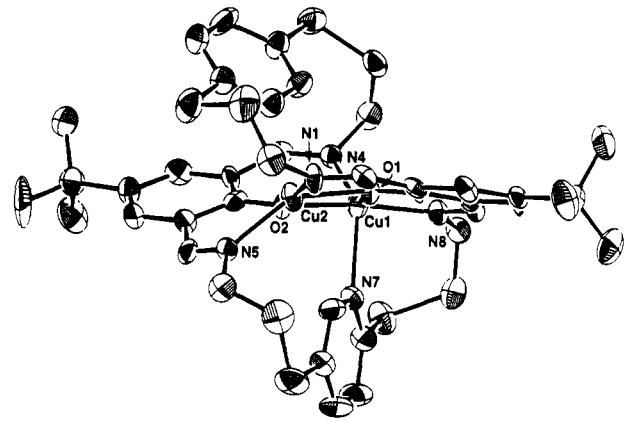

Figure 4. Structural representation of $[Cu_2(M2)]^{2+}$ (cation of III) showing the macrocyclic twist.

Description of the Structure of $[Cu_2(M2)](BF_4)_2 \cdot CH_3OH$ (III). The structure of the $[Cu_2(M2)]^{2+}$ cation is shown in Figure 3 and bond lengths and angles relevant to the copper coordination spheres are given in Table IV. The overall structure of III is very similar to that of I, with the same ligand twist and one pyridazine ring positioned over the dinuclear center, roughly at a right angle to the Cu_2O_2 plane (Figure 4). The short Cu(1)–N(7) separation (2.281 (9) Å) is clearly a bonding contact and is significantly shorter than the equivalent bond in I (dihedral angle between the Cu_2O_2 plane and the pyridazine ring is 100.7°). Cu(1) can, therefore, be considered to have a distorted five-coordinate geometry approaching that of a trigonal bipyramid. Even though the Cu(2)–N(2) separation (2.37 (1) Å) is short enough to be considered as a bonding distance, the twist of this pyridazine ring (dihedral angle of 54.6° with respect to the Cu_2O_2 plane) is such that the N(2) lone pair would not be expected to overlap effectively with the axial copper orbital. Cu(2) is therefore considered to be four-coordinate with significant tetrahedral distortion. The angles at the phenoxide bridges are comparable with those in I, with a slightly larger angle at O(2) (Cu(1)–O(2)–Cu(2) 105.3 (3)°). Solid angles at the phenoxide bridges (O(1) 357.6°, O(2) 358.3°) are close to 360°, indicative of almost planar oxygen centers. The difference in structure between I and III, in particular

Table V. Spectroscopic and Magnetic Data

compound	electronic data λ_{max} (nm) (ϵ (L mol^{-1} cm^{-1}))	μ_{eff}(RT) (μ_B)	g	$-2J$ (cm^{-1})	ρ	TIP (10^6 cgsu)	10^2R
$[Cu_2(M1)](BF_4)_2 \cdot H_2O$ (I)	640, [450], 400[a] 700 (240), [450], 360 (7950)[b]	0.71	2.109 (9)	753 (3)	0.0325	84	1.47
$[Cu_2(M1)](ClO_4)_2$ (II)	640, [450], 390[a] 700 (210), [450], 360 (7500)[b]	0.53					
$[Cu_2(M2)](BF_4)_2 \cdot CH_3OH$ (III)	715, [450], 375[a] 680 (210), 365 (9050)[b]	0.82	2.11 (1)	610 (2)	0.0019	70	0.54
$[Cu_2(M2)](ClO_4)_2 \cdot H_2O$ (IV)	710, [440], 375[a] 710 (210), 365 (8960)[b]	0.88	2.10 (5)	595 (10)	0.008	95	1.22

[a] Mull transmittance. [b] DMF solution; shoulders given in brackets.

concerning the overall ring geometry, may be a reflection, in part, on steric effects associated with the different 4-alkyl substituents.

Both I and III have quite different internal copper ion stereochemistries in the solid state and the unusual close approach of N(2) to Cu(1) in I and N(2) to Cu(2) in III begs the question as to whether the apparent nonalignment of the pyridazine nitrogen lone pairs with respect to an appropriate copper orbital (these would nominally be expected to be in the plane of the pyridazine ring), should be taken to indicate "no" bonding interaction. The bond angles N(1)–Cu(1)–O(2) (163.9 (7)°), N(5)–Cu(1)–O(1) (152.1 (6)°) (I), and N(1)–Cu(2)–O(2) (168.1 (3)°) and N(5)–Cu(2)–O(1) (144.5 (3)°) (III) suggest that these copper centers might experience some axial perturbation due to the presence of the "nonaligned" pyridazine nitrogen.

Spectral and Magnetic Properties. Infrared spectra of all the complexes are very similar, with two characteristic ν(C=N) vibrations in the ranges 1599–1610 and 1623–1625 cm^{-1} and fundamental vibrations associated with perchlorate and tetrafluoroborate indicate of their ionic nature. The electronic spectra are characterized by the presence of a broad band of medium intensity (Table V) at 640–715 nm, in both the solid state and a DMF solution, associated with a d–d transition. Slight shifts in the position of the solid-state band to lower energy in solution are observed for I and II, suggesting a change in stereochemistry, which may be associated with solvent coordination. Any weak axial association of pyridazine nitrogen atoms could be disrupted in solution by a simple twist of the pyridazine groups about the ring carbon–sulfur bonds. Much smaller shifts are observed for III and IV (no shift for IV) indicating that pyridazine coordination is much stronger in these complexes (Cu(1)–N(7) 2.281 (9) Å for III) in keeping with structural data. The shoulder observed in the range 440–450 nm in the solid spectra in solution for I and II is associated with phenolate to copper(II) ligand to metal charge transfer,[45] while the intense absorptions in the range 360–400 nm are tentatively assigned to π–π^* transitions.

Room-temperature magnetic moments for all the dicopper(II) complexes are very low (Table V), indicative of very strong intramolecular antiferromagnetic coupling. Variable-temperature magnetic data have been collected for compounds I, III, and IV in the temperature range 4–300 K and the experimental data for III are given in Figure 5. A sharp rise in susceptibility at low temperatures indicates the presence of uncoupled, paramagnetic impurity, but the pronounced rise above about 100 K is a clear indication of the presence of net antiferromagnetism. The data were fitted to the Bleaney–Bowers expression (eq 1)[46] using the

$$\chi_m = \frac{N\beta^2g^2}{3kT}\left[1+\frac{1}{3}\exp(-2J/kT)\right]^{-1}(1-\rho) + \left[\frac{N\beta^2g^2}{4kT}\right]\rho + N\alpha \quad (1)$$

isotropic (Heisenberg) exchange Hamiltonian ($H = -2JS_1S_2$)

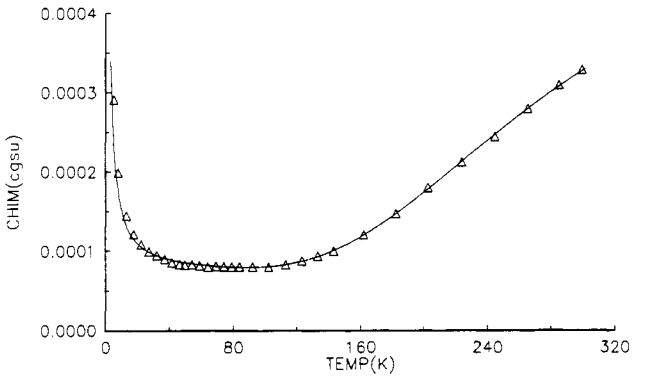

Figure 5. Magnetic data for $[Cu_2(M2)](BF_4)_2$ (III). The solid line was calculated from eq 1 with $g = 2.11$ (1), $-2J = 610$ (2) cm^{-1}, $\rho = 0.0019$, and $N\alpha = 70 \times 10^{-6}$ cgsu ($10^2R = 0.54$).

for two interacting $S = {}^1/_2$ centers (χ_m is expressed per mole of copper atoms, $N\alpha$ is the temperature independent paramagnetism, and ρ is the fraction of monomeric impurity).

A nonlinear regression analysis of the data was carried out with ρ as a floating parameter. The best fit line is shown in Figure 5 for $g = 2.11$ (1), $-2J = 610$ (2) cm^{-1}, $\rho = 0.0019$, $N\alpha = 70 \times 10^{-6}$ cgsu ($10^2R = 0.54$; $R = [\Sigma(\chi_{obs}-\chi_{calc})^2/\Sigma(\chi_{obs})^2]^{1/2}$). The results for similar regression analyses for I and IV are given in Table V.

All three complexes (I, III, and IV) are strongly antiferromagnetically coupled, and the low magnetic moment for II suggests strong coupling also. Spin-exchange occurs via a superexchange mechanism through the phenoxide oxygen bridge network, a feature which has been shown to be responsible for strong antiferromagnetic coupling in many other related complexes. The marked distinction between the exchange coupling constants of I and III warrants some comment. These complexes (I and III) have highly distorted structures when compared with analogous compounds involving e.g. simple aliphatic linkages between the azomethine nitrogen centers. In both compounds a significant axial interaction from a pyridazine nitrogen makes one of the copper centers five-coordinate, albeit severely distorted, while the other copper nominally experiences a significant tetrahedral distortion. The copper–phenoxide (Cu_2O_2) ring in both complexes remains fairly flat and the solid angles at the phenoxide oxygen are all in excess of 357.5°, indicating essentially trigonal, planar oxygens and no significant reduction in exchange as a result of pyramidal character at the oxygen bridge. Copper phenoxide–oxygen distances in I are all in the range 1.90–1.96 Å, comparable with three Cu–O distances in III. The fourth Cu–O distance in III (2.026 (7) Å) is slightly longer, but would not be expected to cause a marked decrease in net antiferromagnetism. Given that the average Cu–O–Cu bridge angle in III (102.8°) is slightly larger than that in I (101.8°) then somewhat larger antiferromagnetic coupling would have been expected for III, other things being considered equal. Also, based on a comparison of exchange as a function of phenoxide bridge angle the magnitude of $-2J$ for I is somewhat smaller than values observed for "normal" macrocyclic complexes of this sort with

(45) Oberhausen, K. J.; Richardon, J. F.; Buchanan, R. M.; McCusker, J. K.; Hendrickson, D. N.; Latour, J.-M. *Inorg. Chem.* **1991**, *30*, 1357.
(46) Bleaney, B.; Bowers, K. D. *Proc. R. Soc. London, A.* **1952**, *214*, 451.

Table VI. Electrochemical Data[a]

compound	electrode	$E^1_{1/2}$ (V)[b]	ΔE_p (mV)[c]	$E^2_{1/2}$ (V)	ΔE_p (mV)	$E^1_{1/2} - E^2_{1/2}$ (mV)	$10^{-9}K_{Con}$[d]
$[Cu_2(M1)](BF_4)_2 \cdot H_2O$ (I)	GC	–0.085	120	–0.64	120	0.56	3.0
	Pt	–0.100	100	–0.65	120		
$[Cu_2(M1)][ClO_4]_2$ (II)	GC	–0.09	120	–0.64	140	0.55	2.0
	Pt	–0.09	120	–0.66	130		
$[Cu_2(M2)][BF_4]_2 \cdot CH_3OH$ (III)	GC	–0.08	105	–0.67	125	0.59	9.6
$[Cu_2(M2)][ClO_4]_2 \cdot H_2O$ (IV)	GC	–0.08	120	–0.66	135	0.58	6.5

[a] *N,N*-Dimethylformamide (DMF) solution with 0.1 M tetraethylammonium perchlorate (TEAP) or tetraethylammonium tetrafluoroborate electrolyte (TEFB). All potentials are referenced to standard calomel electrode (SCE). [b] Scan rate 200 mV/s. [c] Separation between waves ($E_{ox} - E_{red}$) in cyclic voltammograms. [d] $E^1_{1/2} - E^2_{1/2} = 0.0591 \log (K_{con})$.

five- and six-membered chelate rings (N_2Cu), while the value for III is markedly reduced and compares with situations where electron withdrawing effects involving bonded halogens reduce antiferromagnetic exchange.[20] This leaves the geometry at each copper center and therefore the magnetic ground state as the most likely factor to influence exchange significantly.

The long axial contact in I to the pyridazine nitrogen (Cu(2)–N(7) 2.69 (21) Å) appears to have only a minor effect on the geometry at Cu(2), with Cu(2) not displaced significantly from the mean equatorial N_2O_2 plane. Cu(2) appears, therefore, to have a distorted square-pyramidal geometry. Cu(1) has a tetrahedrally distorted square-planar geometry and so both copper atoms are bridged equatorially by magnetically active, nominally $d_{x^2-y^2}$ orbitals. The case for III is somewhat different. Cu(2) realistically adopts a tetrahedrally distorted square-planar geometry, while the close Cu(1)–N(7) (pyridazine) contact (2.281 (9) Å), coupled with the combined angles around Cu(1), indicates that an appropriate geometric description for Cu(1) would be that of a distorted trigonal bipyramid with the Cu(1)–O(2) and Cu(1)–N(8) bonds defining the major axis. The magnetic combination in the geometric limit (i.e. square planar/trigonal bipyramidal) would thus involve a $d_{x^2-y^2}$ copper center and a d_{z^2} copper center, bridged by the two phenoxide oxygens. This would, of necessity, lead to considerably weakened antiferromagnetic exchange, as is observed. However, since the two copper centers in III are still quite strongly coupled it is likely that, at least around Cu(1), a ground state mixing of both $d_{x^2-y^2}$ and d_{z^2} exists. A similar situation is anticipated for IV which has magnetic properties very similar to those of III.

Electrochemistry. The electrochemical properties of the dinuclear Cu(II)–Cu(II) compounds I–IV were studied by cyclic voltammetry in DMF solutions containing 0.1 M tetraethylammonium perchlorate (TEAP) or 0.1 M tetraethylammonium tetrafluoroborate (TEFB) as supporting electrolytes at glassy-carbon and/or platinum working electrodes. Cyclic voltammograms for all the complexes are very similar and involve two quasi-reversible, clearly distinguishable redox processes at negative potentials ($E^1_{1/2}$ = –0.08 to –0.10 V; $E^2_{1/2}$ = –0.64 to –0.67 V (vs SCE)), corresponding to stepwise one-electron reductions through a Cu(II)–Cu(I) intermediate to a dinuclear Cu(I) species. A typical voltammogram for I is deposited (see supplementary material). Data for I–IV, including $E_{1/2}$ values and peak-to-peak separations are given in Table VI. Controlled potential electrolysis experiments in DMF show that in all cases each redox wave is associated with one electron transfer.

The two redox waves are very well separated and conproportionation constants (K_{con}) (eq 2) given in Table VI are substantially

$$[Cu^{II}Cu^{II}L]^{2+} + [Cu^{I}Cu^{I}L] \overset{K_{con}}{\rightleftharpoons} 2[Cu^{II}Cu^{I}L]^{+} \quad (2)$$

larger than those reported for more traditional macrocycle complexes of this sort[14,18,19] involving simple aliphatic linkages between the imine nitrogen centers and copper ions with geometries much closer to square-planar. Flexibility in this linkage appears to be important in terms of the magnitude of both reduction potentials. Changing the aliphatic linkage from propylene to butylene leads to a substantial shift of both reduction waves to positive potentials ($E^1_{1/2}$ = –0.43, $E^2_{1/2}$ = –0.90, propylene (DMSO/SCE); $E^1_{1/2}$ = –0.30, $E^2_{1/2}$ = –0.76, butylene (DMSO/SCE))[14,18] associated with enhanced molecular flexibility. An even more marked shift to positive potentials is observed for both redox waves for I–IV, which is clearly associated not only with the flexibility of the imine bridge linkage but also with the significant tetrahedral distortions present at the copper centers.

Considering the stability of the Cu(II)–Cu(I) intermediates, these one-electron-reduced species should be amenable to study by EPR spectroscopy, to investigate the nature of the interaction of the unpaired electron with the two copper centers. The mixed-valence Cu(II)–Cu(I) species were prepared by controlled-potential electrolysis at –0.4 V (vs SCE), during which the color of the complexes changed from green to dark brown (further reduction at –0.8 V resulted in the transfer of one additional electron equivalent of charge and further color change to deep red).

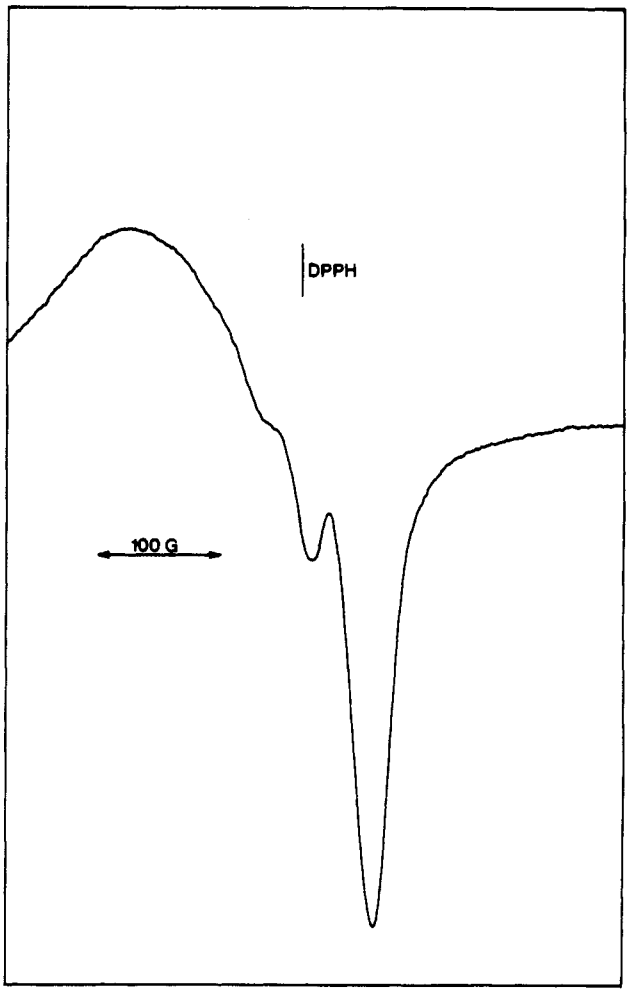

Figure 6. EPR spectrum (X-band) for DMF solution of $[Cu^{II}Cu^{I}(M2)](BF_4)$ (III) (room temperature).

Table VII. X-Band EPR Parameters for Mixed-Valence Cu(II)–Cu(I) Complexes

compound	temp (K)	g_{av}	$g_{\parallel}$	$g_{\perp}$	A_{iso} (10^{-4} cm^{-1})	$A_{\parallel}$ (10^{-4} cm^{-1})
$[Cu^{II}Cu^{I}(M1)][BF_4]$ (I)	295	2.06			38	
	77		2.23	2.04		170
$[Cu^{II}Cu^{I}(M1)][ClO_4]$ (II)	295	2.07			35	
	77		2.23	2.04		170
$[Cu^{II}Cu^{I}(M2)][BF_4]$ (III)	295	2.07			42	
	77		2.22	2.03		172
$[Cu^{II}Cu^{I}(M2)][ClO_4]$ (IV)	295	2.06			45	
	77		2.22	2.02		173

EPR spectra were recorded for all four mixed-valence Cu(II)–Cu(I) complexes in DMF at room temperature (295 K) and at liquid-nitrogen temperature. At room temperature all four spectra are essentially the same. Figure 6 illustrates the spectrum for III, which shows an "axial" signal with some resolved and unresolved hyperfine components. The spectrum is very reminiscent of a one-electron system, where on the EPR time scale the odd electron is largely delocalized over two copper centers.[18,19] From the resolvable hyperfine structure average A_{iso} values are found in the range (35–45) × 10^{-4} cm^{-1} (Table VII), which compare closely with those reported previously for related, delocalized seven-line species.[18,19] In an earlier study of the variable-temperature EPR spectra of related systems with simple, aliphatic, imine bridges Hendrickson and co-workers[19] have shown that the seven-line room temperature spectra gradually disappear as temperature is lowered, to be replaced at low temperatures by four-line spectra typical of localized, one-electron species. The room temperature spectra for I–IV closely resemble the intermediate temperature spectra of these room-temperature delocalized species.

The frozen glass (77 K) spectra of all four mixed-valence state complexes are typical "axial" spectra, with well-resolved copper hyperfine lines in the $g_{\parallel}$ region. The spectrum of I (DMF, 77 K) is shown in Figure 7, and spectral parameters are given in Table VII. In the frozen glass the unpaired electron in each of the four complexes is localized on one copper center. Copper hyperfine ($A_{\parallel}$) splittings fall in the range (170–173) × 10^{-4} cm^{-1} (Table VII), which are somewhat lower than values for related complexes reported by Hendrickson[10,19] ((174–194) × 10^{-4} cm^{-1}), clearly indicating a more pronounced tetrahedral distortion at the copper centers in I–IV, consistent with the structural data.

Conclusion

Template condensation of DFP and PTA, in the presence of copper salts with noncoordinating anions, produces macrocyclic dinuclear copper(II) complexes with the familiar phenoxide bridges and terminal imine nitrogen donors, but with a most unusual molecular twist involving the linking of the imine groups across the dinuclear center, thus presenting the pyridazine nitrogens as potential axial donors. Strong antiferromagnetic coupling and well separated one-electron redox waves are typical for systems of this sort, but the markedly positive one-electron reduction potentials and relatively small $A_{\parallel}$ values in the frozen-glass EPR spectra distinguish compounds I–IV from the normal macrocyclic complexes of this type, in keeping with their highly distorted copper ion geometries.

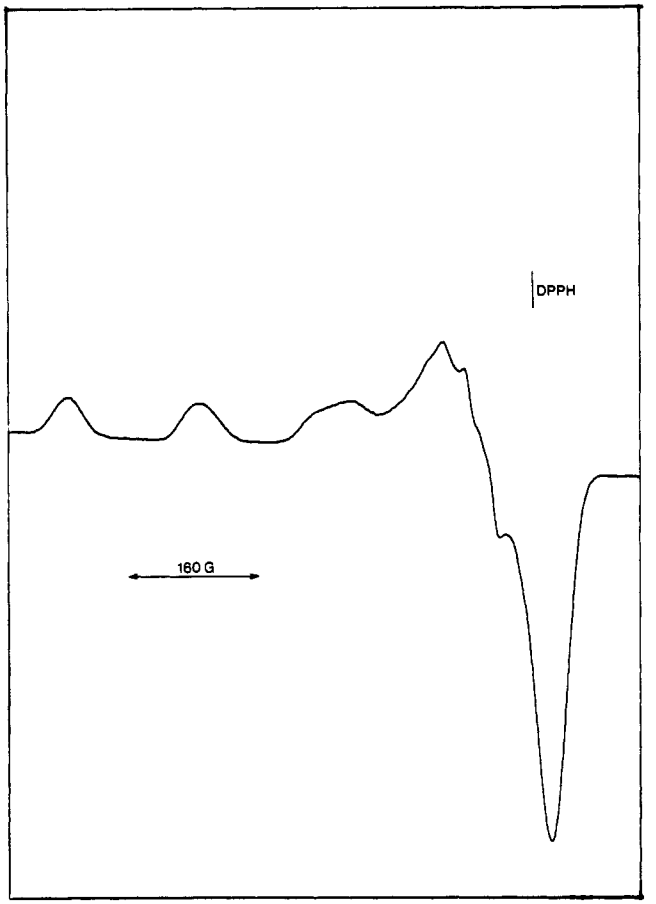

Figure 7. EPR spectrum (X band; frozen glass) for $[Cu^{II}Cu^{I}(M1)](BF_4)$ (I) in DMF (77 K).

Acknowledgment. We thank the Natural Sciences and Engineering Research Council of Canada for financial support for this study.

Supplementary Material Available: A figure showing a cyclic voltammogram for I and tables of hydrogen atom atomic coordinates (Tables SI and SIII), anisotropic thermal parameters (Tables SII and SIV), bond distances and angles (Tables SV and SVI), and least-squares planes (Tables SVII and SVIII) for I and III, respectively (43 pages). Ordering information is given on any current masthead page.